Study on the Stability of Reservoir Slopes with Cavities under Seismic Load

Qingzhao Ren[1,a], Guanzhong Wu[1,2,3,*], Hairui Gou[1,b], Wensong Wang[2,3,c], Shaochi Peng[2,3,d]

[1]China Railway Cultural Heritage rehabilitation Technology Innovation Co., Ltd., Chengdu, China
[2]State Key Laboratory of Geohazard Prevention and Geoenvironment Protection, Chengdu University of Technology, Chengdu, China
[3]School of Environment and Civil Engineering, Chengdu University of Technology, Chengdu, China

[a]970499860@qq.com, [*]15055405095@163.com, [b]695367648@qq.com, [c]wws@cdut.edu.cn, [d]2411759220@qq.com

Abstract. Seismic activity and stress concentration in soil cavities are prone to induce landslides, resulting in surges and overflows that reduce the stability of dam structures, thereby posing a threat to the safety of downstream areas. To analyze the stability of slopes under different water storage conditions and load scenarios, the Shuangjiangkou Hydropower Station was used as a case study. Finite element simulations were conducted to assess slope stability before and after quarry excavation at various reservoir water levels. Failure modes and safety factors for each model were obtained. The results indicate that quarry excavation has a minimal impact on slope stability. As the water level rises, slope stability improves. However, seismic activity significantly reduces the safety factor of the slope, necessitating the use of rock bolts for slope reinforcement. This study provides a simulation basis for determining on-site support plans.

Keywords: Slope stability; Safety factor; Seismic load

1 Introduction

The Jiazhajia Cave preserves valuable mural artifacts and is located 2.8 km from the dam site of the Shuangjiangkou Hydropower Station. Once the dam is completed, the cave will be situated below the normal water level. Additionally, to reduce the dependency on external construction materials, artificial excavation of the material field on the back of the slope will be required (as shown in Figure 1, The slope height-to-width ratio is 1:0.75), leading to changes in the internal stress and structural rigidity of the slope. Under seismic loads, the slope is prone to instability, which could result in the destruction of the cave and severe damage to its cultural relics. Therefore, studying the stability of reservoir slopes containing caves under seismic loads has significant engineering value.

H. Bilgin et al. (eds.), *Proceedings of the 2024 6th International Conference on Civil Engineering, Environment Resources and Energy Materials (CCESEM 2024)*, Advances in Engineering Research 253,
https://doi.org/10.2991/978-94-6463-606-2_32

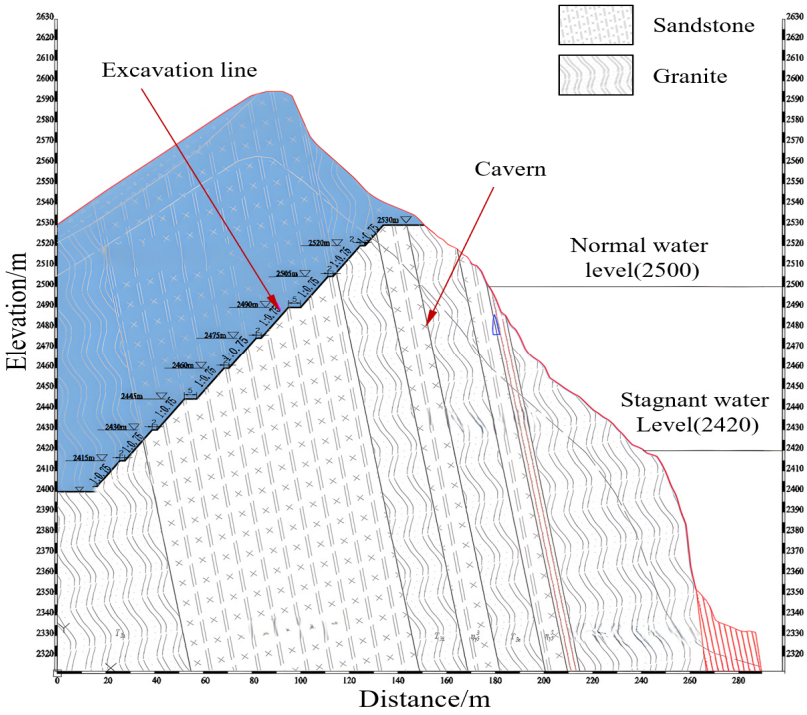

Fig. 1. Side slope cross-section

Numerical simulation and physical experiments are two important methods for studying the impact of seismic loads on slope stability. In numerical simulation, the limit equilibrium method [1-3], strength reduction method [4-6], and dynamic finite element analysis [7-9] are widely used for calculating the safety factor of slopes. With the deeper application of machine learning, parallel optimization methods using unit test simulations are also employed to evaluate the safety factor of slopes under seismic loads [10,11]. In physical model experiments, shaking tables and centrifuges are crucial technical methods for studying slope instability under seismic loads. For example, Yang et al. [12] conducted shaking table tests to investigate the slope instability process under the combined effects of groundwater and seismic activity. Cheng et al. [13] performed dynamic centrifuge model tests under different seismic intensities to study the permanent displacement and failure processes of slopes under varying seismic intensities.

For slopes containing caves, the presence of cavities causes stress concentration, which accelerates the rate of soil failure and reduces the stability of the slope [14]. In response, this study will use the finite element software ABAQUS to construct simulation models under different working conditions to calculate the safety factor of the slope. The aim is to provide a simulation basis for designing support schemes in practical engineering projects.

2 Simulation Scheme Design

2.1 Model Parameters

The lithology of the model is shown in Figure 1. Based on the on-site geological survey report, the mechanical parameters of the rocks are set in the model as shown in Table 1.

Table 1. Rock strength parameters

Material	Density (kg/m^3)	Young's modulus (GPa)	Poisson's ratio	internal friction angle (°)	Cohesion (MPa)
Granite	2620	18	0.23	38.7	1.5
Sandstone	2450	5.5	0.32	28.8	0.6
W-Granite	2620	10	0.26	32	0.9
W-Sandstone	2450	3	0.35	25	0.36

2.2 Simulation Schemes

To analyze the impact of quarry excavation and water storage levels on slope stability, the simulation schemes are designed as shown in Table 2.

Table 2. Simulation schemes

Number	NN1	NS1	EN1	ES1	EN2	ES2	EN3	ES3
Quarry	Non-excavation				Excavation			
Water level	None water				Stagnant water level		Normal water level	
Load	G	Seismic	G	Seismic	G	Seismic	G	Seismic

The initial letter in the numbering represents the quarry excavation condition (N for no excavation, E for excavation). The second letter represents the working condition (N for natural state, S for seismic state). The number represents the water level condition (1 for no water, 2 for stagnant water level, 3 for normal water level).

In the natural state, the slope is only subjected to self-weight stress. Therefore, in the ABAQUS simulation, vertical gravity is applied to simulate this condition, with the gravitational acceleration set to $g=10\ m^2/s$. The seismic direction is considered to be the most dangerous horizontal direction. Based on the local seismic intensity level, the horizontal peak acceleration used is $g_e=0.1g=1\ m^2/s$, while the vertical acceleration remains $g=10\ m^2/s$.

3 Simulation Results

The plastic strain contour plots and displacement contour plots before and after quarry excavation are shown in Figure 2.

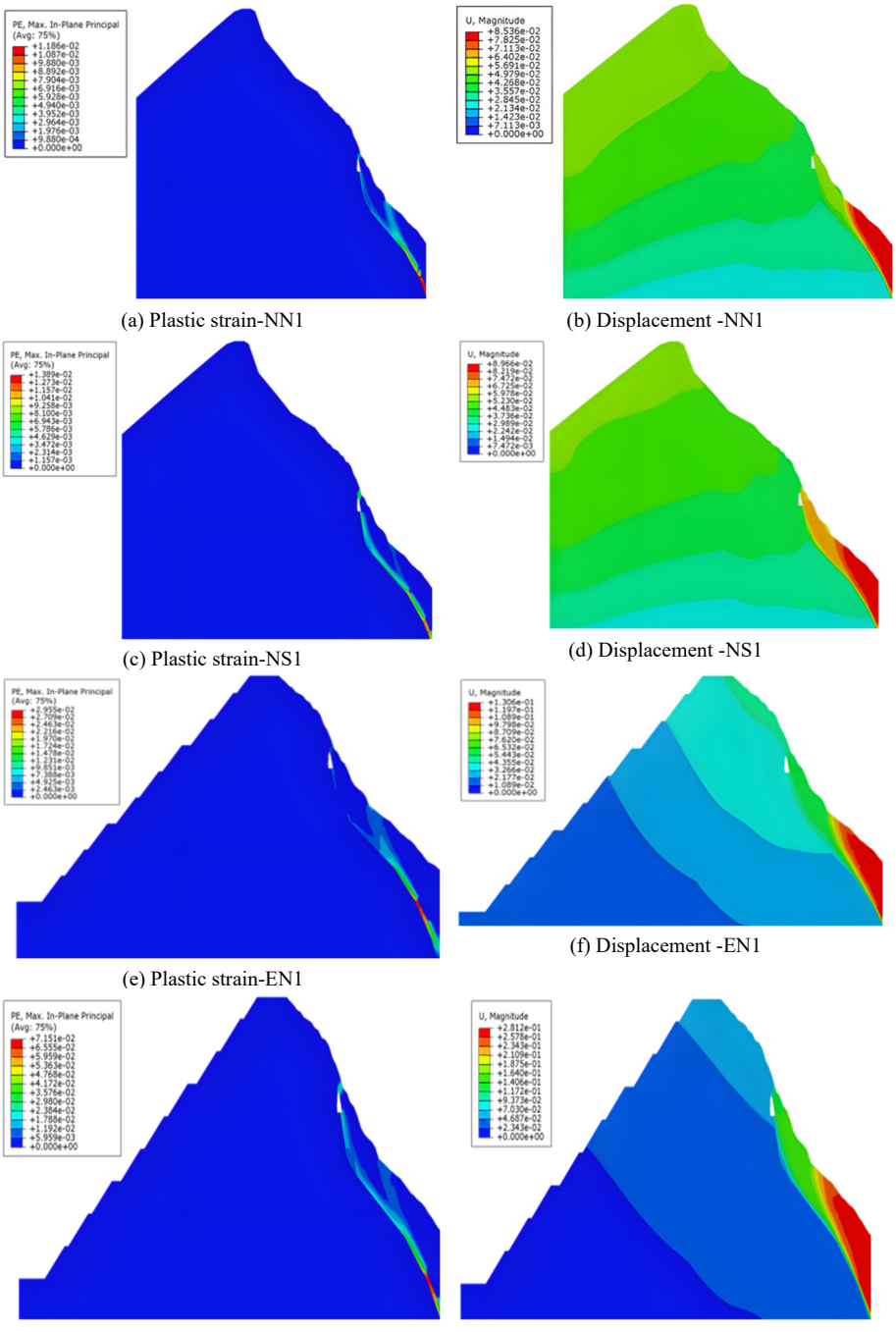

(a) Plastic strain-NN1 (b) Displacement -NN1

(c) Plastic strain-NS1 (d) Displacement -NS1

(e) Plastic strain-EN1 (f) Displacement -EN1

(g) Plastic strain-ES1 (h) Displacement -ES1

Fig. 2. Simulation contour plots before and after quarry excavation

Before quarry excavation, the stability safety factor of the slope under natural gravity conditions is approximately 1.25, and under seismic conditions, it is approximately 1.15. After quarry excavation, the slope safety factor is about 1.24, and the safety factor under seismic load is about 1.13.

Based on the above simulation results, it can be seen that the safety factor of the slope in its natural state is relatively low. When instability occurs, a yield surface connecting the cavities will be generated (as shown in Figure 2a), causing the rock mass below and outside the cavities to slide out (as shown in Figure 2b), thereby having a destructive impact on the cavities. Under seismic conditions, the safety factor of the original slope further decreases, and the yield surface predicted by numerical simulation is similar to that under natural conditions, posing an even greater threat to the safety of the cavities. Therefore, it is necessary to appropriately treat the slopes containing the cavities. It is recommended to reinforce the rock mass in this area using anchor cables penetrating the weathered layer combined with grouting. Additionally, quarry excavation will change the morphology of the original slope, affecting its stress state and altering its stability, thereby reducing the slope stability.

When water enters the strongly weathered rock and soil area, it weakens the structural surface. The rock mass in the weathered layer below the normal water level line is weakened to some extent, and simulation calculations are performed using 60% of the original strength parameters. The simulation contour plots under different water levels are shown in Figure 3.

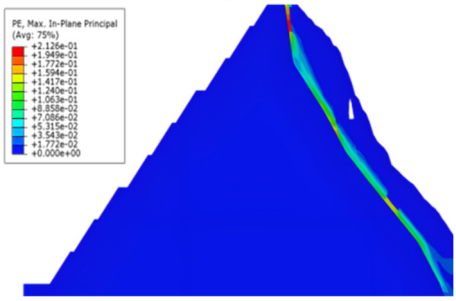

(a) Plastic strain-EN2

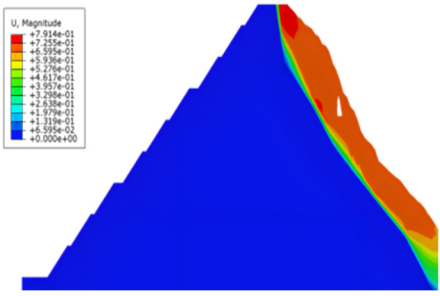

(b) Displacement -EN2

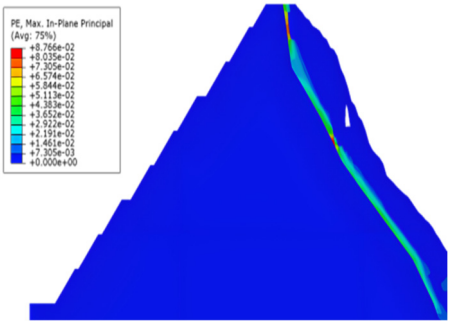

(c) Plastic strain-ES2

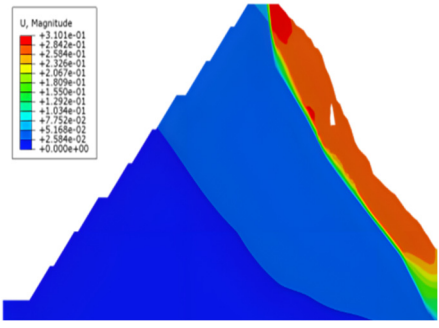

(d) Displacement -ES2

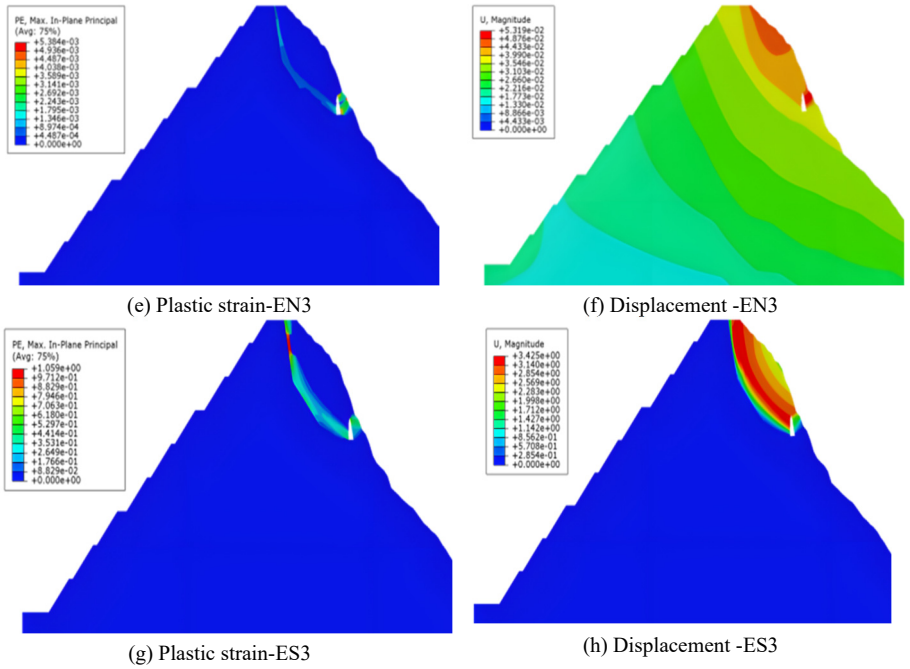

(e) Plastic strain-EN3 (f) Displacement -EN3

(g) Plastic strain-ES3 (h) Displacement -ES3

Fig. 3. Simulation contour plots at different water levels

Under the gravity load, as the water level rises, the slope safety factor increases from 1.35 to 1.38. Under the seismic load, the slope safety factor increases from 1.18 to 1.27. The safety factor of the slope after water storage is higher than before water storage, indicating that the reservoir water pressure helps maintain slope stability in this geological structure. However, once slope instability occurs, the rock mass containing the cavities will be entirely within the sliding body.

At the stagnant water level, the hydrostatic pressure on both sides of the slope is approximately 0.17 MPa and 0.88 MPa. The simulated yield surface in this case is similar to the no-water condition, but the slope safety factor significantly decreases due to seismic activity, greatly increasing the risk to the cavities.

At the normal water level, the hydrostatic pressure on both sides of the slope is approximately 0.96 MPa and 1.7 MPa. In this case, the safety factor is higher, and the reservoir water pressure generated by high water storage improves the stability of the original slope. However, the rock mass near the cavities faces a higher risk of instability, directly affecting the safety of the cavities. The safety factor decreases due to seismic activity, increasing the danger to the cavities.

The above results highlight the necessity of anchor bolt reinforcement. When slope instability occurs, the overall sliding surface is blocked by the anchored reinforcement area, reducing the likelihood of rock mass instability in the area containing the cavities.

4 Conclusion

1. The safety factors and failure contour plots of the slope under the three influencing factors of quarry excavation, water storage, and seismic activity were calculated through numerical simulation.

2. After quarry excavation, the slope stability slightly decreases, while the rise in reservoir water level contributes to the improvement of slope stability.

3. The earthquake has significantly reduced the stability of the slope, in slope stabilization, it is essential to strengthen the support provided by anchors and cables.

This study does not consider the impact of precipitation on slope stability. In actual engineering practice, slope stability is significantly affected by rainfall. Therefore, it is essential to fully consider the effects of precipitation in subsequent analyses.

Acknowledgment

This study was funded by Research projects of C.R.E.C. (2021-key point-34, 2022-key point-01, 2023-major-02).

Reference

1. Du X, Chai J. Stability evaluation of medium soft soil pile slope based on limit equilibrium method and finite element method[J]. Mathematics, 2022, 10(19): 3709. https://doi.org/10.3390/math10193709.
2. Lyu Y, Chen X, Cui L, et al. A Limit Equilibrium Method Based on Geostress Calculated by Implicit Stabilized Node-Based Smoothed Finite Element Method for Stability Analysis of Soil Slopes[J]. Geotechnical and Geological Engineering, 2024: 1-21. https://doi.org/10.1007/s10706-024-02882-6.
3. Azarafza M, Akgün H, Ghazifard A, et al. Discontinuous rock slope stability analysis by limit equilibrium approaches–a review[J]. International Journal of Digital Earth, 2021, 14(12): 1918-1941. https://doi.org/ 10.1080/17538947.2021.1988163.
4. Hua C, Yao L, Song C, et al. Variational method for determining slope instability based on the strength reduction method[J]. Bulletin of Engineering Geology and the Environment, 2022, 81(10): 395. https://doi.org/ 10.1007/s10064-022-02895-6.
5. Wei Y, Hanhua T, Jiandong N, et al. A new criterion for defining the failure of a fractured rock mass slope based on the strength reduction method[J]. Geomatics, Natural Hazards and Risk, 2020, 11(1): 1849-1863. https://doi.org/ 10.1080/19475705.2020.1814428.
6. Chen G, Li H, Wei T, et al. Searching for multistage sliding surfaces based on the discontinuous dynamic strength reduction method[J]. Engineering Geology, 2021, 286: 106086. https://doi.org/ 10.1016/j.enggeo.2021.106086.
7. Barrero A R, Taiebat M, Dafalias Y F. Modeling cyclic shearing of sands in the semifluidized state[J]. International Journal for Numerical and Analytical Methods in Geomechanics, 2020, 44(3): 371-388. https://doi.org/10.1002/nag.3007.
8. Fuentes W, Tafili M, Triantafyllidis T. An ISA-plasticity-based model for viscous and non-viscous clays[J]. Acta Geotechnica, 2018, 13: 367-386. https://doi.org/10.1007/s11440-017-0548-y.

9. Boulanger R W. Nonlinear dynamic analyses of Austrian dam in the 1989 Loma Prieta earthquake[J]. Journal of Geotechnical and Geoenvironmental Engineering, 2019, 145(11): 05019011. https://doi.org/10.1061/(ASCE)GT.1943-5606.0002156.
10. Nitzsche K, Herle I. Strain-dependent slope stability[J]. Acta Geotechnica, 2020, 15: 3111-3119. https://doi.org/10.1007/s11440-020-00971-3.
11. Schmüdderich C, Machaček J, Prada-Sarmiento L F, et al. Strain-dependent slope stability for earthquake loading[J]. Computers and Geotechnics, 2022, 152: 105048. https://doi.org/10.1016/j.compgeo.2022.105048.
12. Yang H, Cui S, Pei X, et al. Multiple earthquake-induced progressive failure of bedding slopes with a saturated weak layer: Shaking table model tests[J]. Soil Dynamics and Earthquake Engineering, 2023, 170: 107906. https://doi.org/10.1016/j.soildyn.2023.107906.
13. Cheng H, Zhou J, Chen Z, et al. A comparative study of the seismic performances and failure mechanisms of slopes using dynamic centrifuge modeling[J]. Journal of Earth Science, 2021, 32(5): 1166-1173. https://doi.org/10.1007/s12583-021-1481-4.
14. Rodrıguez C E, Bommer J J, Chandler R J. Earthquake-induced landslides: 1980–1997[J]. Soil Dynamics and Earthquake Engineering, 1999, 18(5): 325-346. https://doi.org/10.1016/S0267-7261(99)00012-3.